
DecoyDB: A Dataset for Graph Contrastive Learning in Protein-Ligand Binding Affinity Prediction

Yupu Zhang¹ Zelin Xu¹ Tingsong Xiao¹ Gustavo Seabra²

Yanjun Li^{1,2} Chenglong Li² Zhe Jiang^{1*}

¹Department of CISE, University of Florida, Gainesville, FL, USA

²Department of Medicinal Chemistry, University of Florida, Gainesville, FL, USA

{y.zhang1, zelin.xu, xiaotingsong, yanjun.li, zhe.jiang}@ufl.edu
{seabra, lic}@cop.ufl.edu

Abstract

Predicting the binding affinity of protein-ligand complexes plays a vital role in drug discovery. Unfortunately, progress has been hindered by the lack of large-scale and high-quality binding affinity labels. The widely used PDBbind dataset has fewer than 20K labeled complexes. Self-supervised learning, especially graph contrastive learning (GCL), provides a unique opportunity to break the barrier by pre-training graph neural network models based on vast unlabeled complexes and fine-tuning the models on much fewer labeled complexes. However, the problem faces unique challenges, including a lack of a comprehensive unlabeled dataset with well-defined positive/negative complex pairs and the need to design GCL algorithms that incorporate the unique characteristics of such data. To fill the gap, we propose DecoyDB², a large-scale, structure-aware dataset specifically designed for self-supervised GCL on protein-ligand complexes. DecoyDB consists of high-resolution ground truth complexes ($\leq 2.5\text{\AA}$) and diverse decoy structures with computationally generated binding poses that range from realistic to suboptimal (negative pairs). Each decoy is annotated with a Root Mean Squared Deviation (RMSD) from the native pose. We further design a customized GCL framework to pre-train graph neural networks based on DecoyDB and fine-tune the models with labels from PDBbind. Extensive experiments confirm that models pre-trained with DecoyDB achieve superior accuracy, label efficiency, and generalizability.

1 Introduction

Drug discovery is a lengthy and costly endeavor that involves identifying highly potent molecules capable of interacting with specific molecular targets, such as proteins, within the body to treat diseases. Predicting protein-ligand binding affinity is a fundamental task in the early stages of drug discovery [Kitchen *et al.*, 2004], with applications in two critical areas. First, virtual screening and *de novo* design, both key computer-aided drug discovery techniques, depend heavily on this predictive capability to efficiently narrow down promising hit compound binders from a vast chemical space targeting a specific protein [Li *et al.*, 2022b]. Second, it plays a crucial role in further refining these identified molecules to optimize their binding affinities and other properties [Li *et al.*, 2020].

*Corresponding author.

²Code and data are available at: <https://github.com/spatialdatasciencegroup/DecoyDB> and https://huggingface.co/datasets/YupuZ/Decoy_DB.

Classical methods typically employ theory-inspired, fixed functional forms that utilize predefined features extracted from the protein–ligand complex to estimate affinity. Although certain computational techniques such as molecular mechanics/Poisson–Boltzmann or generalized Born surface area (MM/PBSA, MM/GBSA) [Genheden and Ryde, 2015], thermodynamic integration (TI) [Kirkwood, 1935], free energy perturbation (FEP) [Zwanzig, 1954], can offer decent precision, they are computationally intensive and impractical for use in virtual screening.

In recent years, deep learning-based affinity prediction has seen significant improvement [Rezaei *et al.*, 2022; Zhang *et al.*, 2024], with models utilizing 3D convolutional neural networks (CNNs) [Stepniewska-Dziubinska *et al.*, 2018b; Li *et al.*, 2019] and graph neural networks (GNNs) [Lim *et al.*, 2019; Yang *et al.*, 2023] to represent ligands and proteins and capture structural information. Despite these advances, the accuracy of current scoring functions remains unsatisfactory, and further improvements are hindered by the limited availability of ground truth protein–ligand binding affinity labels. For instance, the widely used PDBbind dataset [Wang *et al.*, 2005] contains fewer than 20,000 labeled complexes. Such labels are typically obtained through laborious and time-consuming experiments and thus are unlikely to grow dramatically. In contrast, there is an abundance of unlabeled protein–ligand complexes in structural databases, which could potentially enhance the learning of spatial structural interaction features for binding affinity prediction.

Self-supervised learning (e.g., masked autoencoder, contrastive learning) has shown great promise in pre-training a deep neural network model based on vast unlabeled samples and fine-tuning the model with limited labels for various downstream tasks, such as natural language processing [Radford *et al.*, 2018] and computer vision [He *et al.*, 2022]. Among these methods, contrastive learning has been proven to be a promising framework for unlabeled graph data [He *et al.*, 2020; Chen *et al.*, 2020], particularly for protein–ligand complexes [Luo *et al.*, 2024]. Motivated by this, we explore contrastive learning as a pre-training strategy to leverage large-scale unlabeled complexes. The resulting model can then be fine-tuned on small labeled datasets to achieve accurate binding affinity prediction.

However, there are several unique challenges. First, there is a lack of a comprehensive unlabeled dataset with well-defined positive/negative complex pairs, which is required for contrastive learning. Second, maintaining the original structural information of protein–ligand complexes is crucial for preserving biochemical constraints. Thus, common graph contrastive learning methods (e.g., using graph perturbations like node or edge dropping to generate positive and negative pairs) [Chen *et al.*, 2020; Wang and Qi, 2022] can potentially generate unrealistic conformations that violate molecular physical and chemical constraints [Qin *et al.*, 2024]. Third, our downstream task of binding affinity prediction requires the neural network to capture binding affinity corresponding to a local minimum energy, which is not considered by typical contrastive learning [Liu *et al.*, 2023].

To fill the gap, we propose *DecoyDB*, a comprehensive dataset of high-resolution ground truth 3D protein–ligand complexes filtered from PDB, augmented by diverse decoy complexes with computationally generated binding poses that range from realistic (positive pairs) to suboptimal (negative pairs). *DecoyDB* consists of 61,104 ground truth 3D complexes and 5,353,307 decoys. Each decoy is annotated with a Root Mean Squared Deviation (RMSD) from the native pose. We also design a customized graph contrastive learning algorithm with: (1) a two-category graph contrastive loss with both continuous negative pair sampling from decoys and discrete negative pairs from different real complexes; and (2) a denoising score matching (DSM) based regularization in the loss. Extensive experiments show that our pre-training framework enhances base models in prediction accuracy, sample learning efficiency, and generalizability. It is worth noting that although we focus on enhancing binding affinity prediction, *DecoyDB* has the potential for broader applications, such as molecular docking and virtual screening.

2 Related Work

Deep Learning for Protein-Ligand Binding Affinity Prediction: In recent years, deep learning has emerged as a powerful tool for predicting protein–ligand binding affinity. Earlier methods are mostly based on CNNs, including Pafnucy [Stepniewska-Dziubinska *et al.*, 2018b], OnionNet [Zheng *et al.*, 2019], and DeepAtom [Li *et al.*, 2019], which typically rasterize the binding pocket and ligand into a grid structure. However, these methods are inherently dependent on the grid resolution and do not consider the topological structure of a complex. In addition, some methods for drug target affinity prediction, such as DeepDTA [Lennox *et al.*, 2021] and GraphDTA [Nguyen *et al.*, 2020],

Table 1: Public datasets related to protein–ligand complexes for binding affinity prediction

Category	Dataset	# of complexes	3D structure	Affinity	Measurement
Both affinity labels and 3D structure	PDBbind2013	10,370	Exp.	Exp.	IC_{50}, K_d, K_i
	PDBbind2016	13,189	Exp.	Exp.	IC_{50}, K_d, K_i
	PDBbind2020	19,443	Exp.	Exp.	IC_{50}, K_d, K_i
	MISATO	19,443	Exp.+QC+MD	Exp.	IC_{50}, K_d, K_i
	LP-PDBbind	18,795	Exp.	Exp.	IC_{50}, K_d, K_i
	BDB2020+	115	Exp.	Exp.	IC_{50}, K_d, K_i
	HiQBind	32,275	Exp. + Refined	Exp.	IC_{50}, K_d, K_i
	Binding MOAD	41,409	Exp.	Exp.	IC_{50}, K_d, K_i
	BioLip	48,291	Exp.	Exp.	IC_{50}, K_d, K_i
	BindingNet	69,816	Exp.+Comp.	Exp.	IC_{50}, K_d, K_i
Only affinity labels, no 3D structure	KIBA	117,657	-	Exp.	KIBA (IC_{50}, K_d, K_i)
	Davis	30,056	-	Exp.	K_d
	BindingDB	679,000	-	Exp.	IC_{50}, K_d, K_i
No affinity labels, only 3D structure	PDB (05/2025)	178,900	Exp.	-	-
	Redocked 2020	786,960	Exp. + Decoys	-	-
	DecoyDB	5,414,411	Exp. + Decoys	-	-

miss the interaction structures. Recent works have shifted towards graph neural networks (GNNs) to learn a flexible representation of 3D graph structures, such as PotentialNet [Feinberg *et al.*, 2018], IGN [Jiang *et al.*, 2021], EGNN [Satorras *et al.*, 2021], and GIGN [Yang *et al.*, 2023].

Graph Contrastive Learning: Generic graph contrastive learning (GCL) generates positive and negative sample pairs via random node dropping, perturbation, or subgraph sampling [You *et al.*, 2020; Xu *et al.*, 2021; Tong *et al.*, 2021], which tend to destroy biochemical properties. Although recent advances have introduced GCL specifically for molecular data [Guan and Zhang, 2023; Fang *et al.*, 2023; Liu *et al.*, 2022; Sun *et al.*, 2021; Li *et al.*, 2022a], these models often focus on a single molecular graph and fail to incorporate the interactions between protein and ligand graphs. Wu *et al.* [Wu *et al.*, 2022] proposes a self-supervised learning method but requires extra molecular dynamics simulation. Ni *et al.* [Ni *et al.*, 2024] also evaluates their molecular foundation model on protein-ligand binding affinity prediction, but their base model was pre-trained on single molecules. Luo *et al.* [Luo *et al.*, 2024] proposes a self-supervised learning method for protein-ligand binding with a contrastive loss based on negative sample pairs from decoys. However, the complexes in their pretraining dataset were derived from PDBbind, i.e., the same complexes are used for pretraining and fine-tuning. In addition, their contrastive loss does not consider different extents of negativity of decoys with varying deviations.

Protein-ligand complex datasets: Table 1 summarizes the existing public protein-ligand complex datasets. Most datasets are derived from the Protein Data Bank (PDB) [Berman *et al.*, 2000], a comprehensive repository of experimentally determined 3D biomolecular structures. PDB (as of 05/2025) provides around 178,900 protein-ligand complexes but does not provide binding affinity labels. To fill the gap, PDBbind provides fewer than 20K complexes with experimentally measured affinity and is the most widely used benchmark for binding affinity prediction. Several datasets aim to enrich or refine the PDBbind with additional structural or physical information. For example, MISATO [Siebenmorgen *et al.*, 2024] augments PDBbind entries with quantum-chemically (QC) optimized ligand geometries and 10-nanosecond molecular dynamics (MD) trajectories. LP-PDBbind [Li *et al.*, 2024a] provides a leakage-proof split of PDBbind based on structural information. In addition, the authors construct a high-quality test set, BDB2020+, by selecting new protein-ligand complexes published after PDBbind2020 for independent testing. There are several additional labeled datasets. Binding MOAD [Wagle *et al.*, 2023] provides 41,409 complexes, of which only 15,223 (37%) are annotated with affinity labels. BioLiP [Yang *et al.*, 2012] integrates Binding MOAD, PDBbind, and BindingDB, providing over 48,000 labeled complexes, but it does not apply resolution filtering and thus can contain low-quality 3D complex structures. HiQBind [Wang *et al.*, 2025] collects 32,275 protein-ligand complexes with refined structures. Despite their high-quality affinity labels, these datasets remain relatively small in scale, and there exist substantial overlaps between them. For example, BioLiP shares 26,009 complexes with Binding MOAD, and most complex structures in HiQBind are from Binding MOAD and BioLiP. To support larger-scale labels, BindingNet [Li *et al.*, 2024b] expands PDBbind to 69,816 complexes by superimposing ligands in the original complexes. However, since the 3D structures are computationally generated, potential mismatches may exist between the complex structures and the corresponding binding affinity. Separately, several other datasets such as KIBA [Tang *et al.*, 2014], Davis [Davis *et al.*, 2011], and BindingDB [Liu *et al.*,

2007] provide a larger number of binding affinity labels, but they do not provide corresponding 3D conformal structures. In summary, most existing datasets are designed exclusively for supervised learning and therefore cannot leverage the vast number of unlabeled 3D complexes. One existing dataset, Redocked2020 [Francoeur *et al.*, 2020], augments 3D complexes in PDBbind to 786,960 binding poses by adding decoys (via redocking ligands into protein structures) for self-supervised pretraining based on graph contrastive learning [Luo *et al.*, 2024]. However, since the 3D complexes are entirely derived from PDBbind, there exists leakage between pretraining and fine-tuning. In contrast, our DecoyDB is filtered from PDB with many complexes outside the PDBbind dataset, providing an opportunity to validate the generalizability of pretrained models during fine-tuning.

3 Problem Definition

Definition 1. A *protein-ligand complex* is a binding interaction between a protein and a ligand. It can be represented as $s_k = (G_k, \mathbf{x}_k, \mathbf{a}_k)$, where $G_k = (V_k, E_k)$ is a 3D graph whose nodes ($v \in V_k$) are atoms of the protein and the ligand, and whose edges ($e \in E_k$) can be chemical interactions between atoms within the protein, within the ligand, or between the protein and the ligand (interactive edges). $\mathbf{x}_k \in \mathbb{R}^{|V_k| \times l}$ is the matrix of node spatial features (e.g., 3D coordinates). $\mathbf{a}_k \in \mathbb{R}^{|V_k| \times m}$ is the matrix of node non-spatial features (e.g., type of atom). $y_k \in \mathbb{R}$ denotes the binding affinity score associated with the complex, which is not available in an unlabeled dataset.

The problem of protein-ligand binding affinity prediction can be formally defined as follows:

Input:

- A set of protein-ligand complexes $\mathcal{S} = \{s_k | 1 \leq k \leq K\}$.
- A small subset of ground truth binding affinity scores $\mathcal{Y} = \{y_k | 1 \leq k \leq K_l\}$, where $K_l \ll K$.
- A base GNN encoder f_θ and regression head g_ϕ : $\hat{y}_k = g_\phi(f_\theta(s_k))$

Output:

- Parameters θ of pre-trained GNN encoder f_θ based on \mathcal{S} .
- Parameters ϕ in regression head g_ϕ based on \mathcal{Y} .

Objective:

- Minimize the prediction errors of the fine-tuned model.
- Maximize the sample efficiency in fine-tuning.

4 Our DecoyDB Dataset

4.1 The Construction of DecoyDB

In order to use unlabeled complexes in self-supervised learning (graph contrastive learning), we need to first establish positive and negative sample pairs. Common data augmentation methods in general graph contrastive learning (e.g., edge perturbation, node dropping) are inadequate since they destroy biochemical structures. Thus, we constructed a specialized dataset to augment the original protein-ligand complexes with decoys. A decoy refers to an artificial protein-ligand complex with a computationally generated suboptimal binding pose. We name our augmented dataset *DecoyDB*.

Figure 1 illustrates our data construction process. We started by retrieving all available structures containing ligand-protein complexes from the PDB, focusing on entries obtained by X-ray crystallography with a resolution of 2.5Å or less. We refined our *DecoyDB* dataset by excluding complexes with ligands that had molecular weights outside the (50, 700) range, metal clusters, monoatomic ions, common crystallization molecules, and ligands containing elements other than C (carbon), N (nitrogen), O (oxygen), H (hydrogen), S (sulfur), P (phosphorus), or X (halogens). To avoid redundancy and irrelevant protein chains, we isolated the target ligand in each remaining PDB entry and retained only those protein chains with at least one atom within 10Å of the ligand and saved a PDB file containing only the protein and ligand. This threshold captures relevant interactions, while excluding distant, noninteracting parts of the protein. In cases where multiple ligands were present within a complex, we generated a separate PDB file for each ligand-protein pair. We collected 63,837 3D complexes after the split.

To generate decoy complexes, we used AutoDock Vina 1.2 [Eberhardt *et al.*, 2021], one of the most widely used open-source programs for molecular docking. For each PDB file (a real protein-ligand

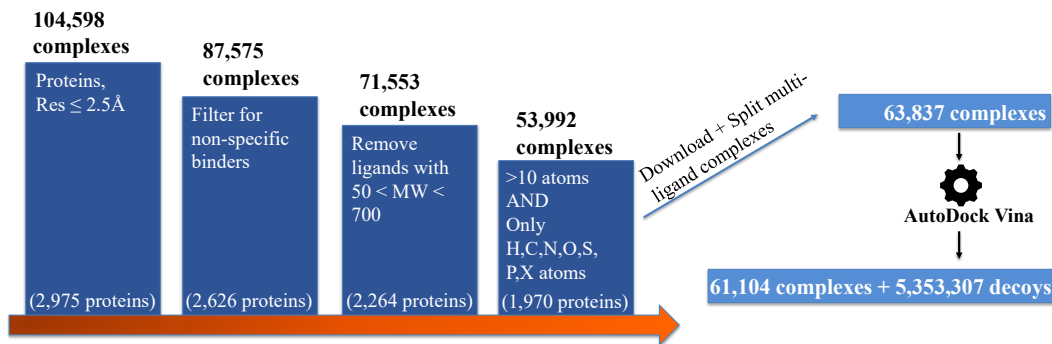


Figure 1: The data construction pipeline of DecoyDB.

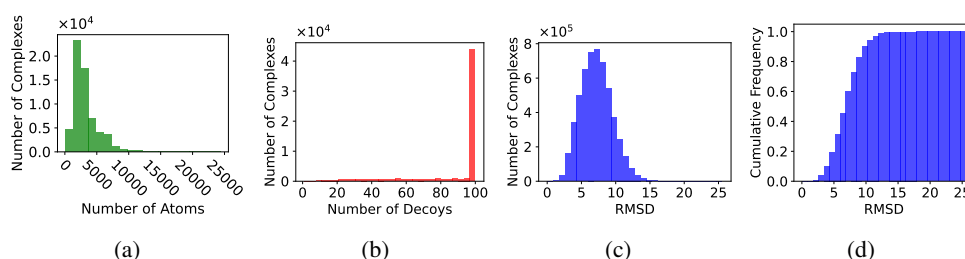


Figure 2: Statistical analysis of *DecoyDB*. (a) Distribution of the number of atoms in each protein-ligand complex. (b) Distribution of the number of decoys per complex. (c) Distribution of RMSD values for decoy complexes. (d) Cumulative distribution of RMSD values for decoy complexes.

complex), we defined a grid box around the ligand with a 5\AA padding in each dimension to ensure sufficient space for ligand flexibility during redocking. We generated 100 different poses per ligand using an exhaustiveness parameter of 8, which balances computational efficiency with pose diversity. The final **Root Mean Square Deviation (RMSD)** between the generated pose and the original crystallized ligand was calculated to quantify the deviation of the decoys from the native binding pose. The RMSD is defined by the spatial distances between the atoms of the decoy’s ligand and the corresponding atoms in the original ligand.

The resulting *DecoyDB* dataset contains 61,104 protein-ligand complexes and 5,353,307 decoys, with an average of 88 successfully generated decoys per complex. The data distribution is shown in Figure 2. The RMSD of the decoys ranges from 0.03\AA to 25.56\AA , with an average of 7.22\AA . This wide range of RMSD values ensures a diverse set of decoys that represent both near-native (**positive pairs**, $\text{RMSD} \leq 2\text{\AA}$) and far-from-native poses (**negative pairs**, $\text{RMSD} > 2\text{\AA}$). Such diversity is crucial for contrastive learning, as it allows the model to learn from a broad range of binding interactions and spatial conformations, improving its generalization in predicting protein-ligand binding affinity.

4.2 A Customized Graph Contrastive Learning Framework

We now introduce a customized graph contrastive learning framework that pre-trains a neural network based on two-category negative sample pairs and denoising-based regularization.

Two-category Graph Contrastive Loss with Continuous Negative Samples

The *DecoyDB* dataset augments the original unlabeled complexes with positive and negative sample pairs. Since we have the RMSD values of negative decoys, we know the extent of the negativity of those negative pairs. We call these continuous negative samples (since they are not binary), which need to be captured in our contrastive loss. In addition to decoys, we define another category of

negative sample pairs based on different real complexes. In other words, for each real complex, other real complexes different from itself are negative pairs.

Our proposed two-category InfoNCE contrastive loss is in Equation 1, where \mathbf{z}_k is the embedding of a real complex (the *anchor*) from the encoder, and \mathbf{z}_i is the embedding of one positive sample, \mathbf{z}_j is the embedding of a negative sample, and N is the total number of samples in the minibatch.

$$l_{k,i} = -\log\left(\frac{\exp(\text{sim}(\mathbf{z}_k, \mathbf{z}_i^T/\tau))}{\sum_{j=1, j \neq i}^N \beta_{k,j} \exp(\text{sim}(\mathbf{z}_k, \mathbf{z}_j^T/\tau))}\right) \quad (1)$$

One important factor in the above loss is $\beta_{k,j}$. It is defined in Equation 2, where $d_{\mathbf{z}_k, \mathbf{z}_j}$ is the RMSD between embeddings \mathbf{z}_k and \mathbf{z}_j , d_{max} is the max RMSD between the real complexes and their decoys (to normalize $d_{\mathbf{z}_k, \mathbf{z}_j}$), sim is the cosine similarity function, and α is a hyper-parameter to balance the relative weight between two categories of negative samples. Specifically, if the negative sample \mathbf{z}_j is from a decoy, we use a normalized continuous RMSD to reflect the extent of negativity in the contrastive loss. For decoys that have more deviations from the anchor complex, our intuition is that their embeddings need to be pushed away further from the anchor. If the negative sample \mathbf{z}_j is from a different complex (than the current anchor complex), then we use a binary weight $\beta = 1$.

$$\beta_{k,j} = \begin{cases} \alpha \frac{d_{\mathbf{z}_k, \mathbf{z}_j}}{d_{max}} & \text{if } \mathbf{z}_j \text{ is a negative decoy of } \mathbf{z}_k, \\ 1 & \text{otherwise.} \end{cases} \quad (2)$$

Suppose there are K anchors in the complex dataset and each anchor has m positive pairs. The loss function L_1 is a sum over all complexes and their positive pairs:

$$L_1 = \frac{1}{m \times K} \sum_{k=1}^K \sum_{i=1}^m l_{k,i} \quad (3)$$

Denoising-based Regularization

Although the above two-category graph contrastive loss helps supervise the relative closeness of embedding pairs, it does not reflect the fact that each real complex has a binding pose with minimum energy. Inspired by a recent work [Jin *et al.*, 2024], we add a denoising-based regularization method. Our intuition is that the real complex structure is the most stable structure and represents the local minimum potential energy in its pose.

Specifically, we add Gaussian noise to the 3D coordinates of atoms in the complex to get perturbed complex $s' = (G, \mathbf{x}', \mathbf{a})$, i.e., $\mathbf{x}' = \mathbf{x} + \epsilon$, where $\epsilon \sim p(\epsilon) = \mathcal{N}(0, \sigma^2 I)$, \mathbf{x} are the coordinates of the atoms and \mathbf{x}' are perturbed coordinates of atoms. Note here we only add Gaussian noise to the ligand atoms. For simplicity, we reuse the same symbol of \mathbf{x} to represent the coordinates of a ligand. The model’s output denotes the structural energy. Our intuition is that the gradient of the model’s score with respect to the input vanishes in the absence of noise. Specifically, **denoising score matching (DSM)** loss based on [Zaidi *et al.*, 2023] is:

$$L_2 = \mathbb{E}_{q_\sigma(\mathbf{x}', \mathbf{x})} \left[\frac{\partial \log f(s')}{\partial \mathbf{x}'} - \frac{\mathbf{x} - \mathbf{x}'}{\sigma^2} \right] \quad (4)$$

where $q_\sigma(\mathbf{x}', \mathbf{x})$ is the joint distribution of perturbed and non-perturbed structures.

To optimize the performance on the prediction task, we integrate contrastive learning with noise-based regularization by combining two different constraints to formulate the overall objective function:

$$L = L_1 + \mu L_2 \quad (5)$$

Here, μ is a hyper-parameter adjusted to balance the contribution of contrastive learning with DSM-based regularization.

5 Experiments

Dataset description: For the pre-training phase, we used the proposed *DecoyDB* dataset and removed overlapping samples from fine-tuning binding affinity datasets. For other pre-training

methods, Frad and ConBAP, we used the pre-training model provided by the authors. Specifically, Frad was pre-trained on PCQM4Mv2 [Nakata and Shimazaki, 2017] and ConBAP was pretrained on Redocked2020 [Francoeur *et al.*, 2020]. For fine-tuning, we used the PDBbind2016 and PDBbind2013 datasets [Wang *et al.*, 2005], which contain 13,189 complexes and 10,370 complexes, respectively. Each sample is associated with a binding affinity. Note that we conduct pretraining only on GNN-based models. For other models, we train them directly on the PDBbind dataset without self-supervised pretraining. To ensure a fair comparison during fine-tuning, we followed the established setup by randomly selecting 11,904 training and 1,000 validation complexes for PDBbind2016, and 7,977 training and 1,000 validation complexes for PDBbind2013. For model testing, we used two independent benchmark test sets: the PDBbind2013 coreset and PDBbind2016 coreset, containing 107 and 285 complexes, respectively. These test sets are also removed from our pre-training dataset to conduct a rigorous evaluation of our pre-training framework.

Evaluation metrics: During pre-training, we used the EarlyStop strategy based on training and validation loss. During fine-tuning, we assessed the model’s test performance using Root Mean Square Error (RMSE) and Pearson’s correlation coefficient (R), following previous works [Stepniewska-Dziubinska *et al.*, 2018a; Zheng *et al.*, 2019].

Baselines: The baseline models include: Docking method (**AutoDock Vina** [Eberhardt *et al.*, 2021]), Drug-Target Affinity methods (**DeepDTA** [Lennox *et al.*, 2021], **GraphDTA** [Nguyen *et al.*, 2020]), CNN-based methods (**Pafnucy** [Stepniewska-Dziubinska *et al.*, 2018b], **OnionNet** [Zheng *et al.*, 2019]), GNN-based methods (**SchNet** [Schütt *et al.*, 2017], **EGNN** [Satorras *et al.*, 2021], **GIGN** [Yang *et al.*, 2023]), General GCL with edge perturbation on GIGN (**GIGN + GCL-EP**), GCL with node dropping on GIGN (**GIGN + GCL-ND**) and **Pre-training for biochemistry graphs (Frad** [Ni *et al.*, 2024], **ConBAP** [Luo *et al.*, 2024]). We compare our customized GCL algorithm (named **OURS**) on DecoyDB against baselines. More details are provided in Appendix B.

Implementation details: For baseline models, we used the original source code provided by the authors. For the pre-training methods, we used the pre-trained model parameters provided by the authors and fine-tuned them on our dataset, where ConBAP used EGNN as its base model, and Frad used TorchMD-Net [Thölke and De Fabritiis, 2022] as its base model. Our pre-training framework used these GNNs as the base encoders for complexes, with two separate dense layers during the pre-training and fine-tuning phases to make predictions. We used GIGN as the base model for the ablation study, sensitivity analysis, the impact of dataset size and the model generalization.

We used the same learning rate ($5e-4$) and weight decay ($1e-6$) for each model in two phases. During the pre-training phase, we trained each model for 20 epochs (Figure 4 (a)). In the fine-tuning phase, each model was trained for a maximum of 300 epochs, with early stopping applied if there was no improvement on the validation set within 40 epochs. The detailed setup can be found in our supplementary materials. All experiments were executed on an NVIDIA DGX-2 node with AMD EPYC 7742 64-core CPU and eight A100 GPUs. We ran each model five times to obtain the average performance and standard deviations. Additional experimental details are provided in Appendix A.

5.1 Overall Performance

Table 2 summarizes the detailed comparison of our framework against baseline models on two datasets. Among the baselines, DTA-based methods show relatively high RMSE values, likely because they do not take into account the detailed spatial structures related to binding interactions. CNN-based models show moderate improvements, with reduced RMSE and increased R values, but their reliance on volume-based representations cannot capture the graph structural information. In contrast, GNN-based models, such as EGNN and GIGN, outperform other baselines, even without pre-training. Particularly, GIGN achieves the best accuracy among all base models. We also compared our pre-training framework with alternative contrastive learning methods (when their source codes were available) on several GNN base models. Results show that adding our pre-training framework significantly improves the base model performance. For instance, on the EGNN base model, our pre-training framework (OURS) reduces the RMSE from 1.304 to 1.250 on the PDBbind 2016, while the existing ConBAP method (which also uses decoys to augment negative samples) only reduces the RMSE to 1.285. As another example, our pre-training method reduces the RMSE of GIGN (the best base model) from 1.460 to 1.386 on the PDBbind core set 2013 and from 1.263 to 1.188 on the PDBbind core set 2016. In contrast, general GCL does not show significant improvement on GIGN.

Table 2: Performance comparison on PDBbind core set 2013 and PDBbind core set 2016

Method		Pretraining dataset	PDBbind core set 2013		PDBbind core set 2016	
			RMSE ↓	R ↑	RMSE ↓	R ↑
Docking	AutoDock Vina	-	2.400	0.570	2.350	0.600
DTA	DeepDTA	-	1.603 (0.014)	0.717 (0.016)	1.366 (0.011)	0.777 (0.013)
	GraphDTA	-	1.742 (0.039)	0.673 (0.032)	1.543 (0.033)	0.707 (0.021)
CNN	Pafnucy	-	1.544 (0.024)	0.778 (0.013)	1.423 (0.040)	0.793 (0.023)
	OnionNet	-	1.562 (0.071)	0.747 (0.031)	1.421 (0.069)	0.772 (0.024)
GNN +pretrain	TorchMD-Net	-	1.466(0.034)	0.763(0.016)	1.294 (0.026)	0.808 (0.011)
	+Frad	PCQM4Mv2	1.447 (0.016)	0.780 (0.008)	1.264 (0.043)	0.811 (0.006)
	SchNet	-	1.662(0.074)	0.727 (0.030)	1.471 (0.019)	0.758 (0.017)
	+OURS	DecoyDB	1.626(0.056)	0.763 (0.026)	1.434 (0.051)	0.779 (0.024)
	EGNN	-	1.508(0.046)	0.774 (0.019)	1.304 (0.033)	0.807 (0.014)
	+ConBAP	Redocked 2020	1.427 (0.047)	0.786 (0.014)	1.285 (0.022)	0.814 (0.016)
	+OURS	DecoyDB	1.417 (0.028)	0.790 (0.013)	1.250 (0.017)	0.817 (0.022)
	GIGN	-	1.460 (0.050)	0.787 (0.024)	1.263 (0.020)	0.814 (0.006)
	+ GCL-EP	DecoyDB	1.455 (0.006)	0.794 (0.021)	1.283 (0.015)	0.812 (0.011)
	+ GCL-ND	DecoyDB	1.467 (0.016)	0.700 (0.008)	1.268 (0.043)	0.819 (0.006)
+OURS	DecoyDB	1.386 (0.043)	0.801 (0.011)	1.188 (0.022)	0.840 (0.008)	

5.2 Sensitivity Analysis

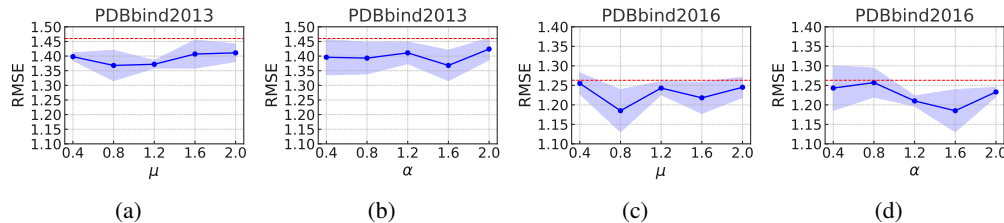


Figure 3: Sensitivity analysis of two key hyper-parameters, α and μ , in our loss function, as shown in Equation 2 and Equation 5. (a) and (c) show the RMSE performance across different values of μ on the two datasets, PDBbind2013 and PDBbind2016. (b) and (d) show the RMSE variation with different values of α on the same two datasets. The red dashed lines show the baseline GIGN model.

In this section, we evaluate the impact of two key hyperparameters α and μ . α (Equation 2) influences the relative weight of the factor β (i.e., relative weight of decoy negative samples versus negative samples from different complexes), while μ balances the relative weight of contrastive learning and DSM. We varied both parameters ranging from 0.4 to 2.0 and observed variations in RMSE across the test datasets. As shown in Figure 3, RMSE initially decreases and then increases with rising α , but it is persistently lower than the RMSE of the baseline GIGN model (shown as the red dashed line). The results of μ follow a similar trend.

5.3 Ablation Study

Our ablation study evaluates the impact of two key modules, i.e., the graph contrastive learning (GCL) and denoising score matching (DSM)-based regularization in the pre-training phase. We used GIGN as the base model, starting with a full framework that included both components and then removing each component to observe the impact on model performance. As shown in Figure

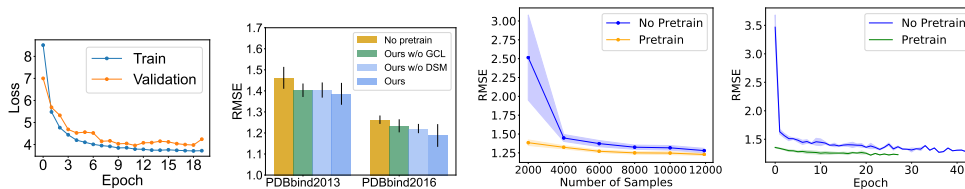


Figure 4: (a) is the training and validation loss curve during pre-training. (b) is the ablation study. (c) is the impact of fine-tuning dataset size on the binding affinity prediction. (d) is the validation curve in fine-tuning

Table 3: Ablation study on our two-category graph contrastive loss

Method	core set 2013	core set 2016
with one-category graph contrastive loss	1.406(0.047)	1.246(0.014)
with two-category graph contrastive loss	1.394(0.036)	1.221(0.022)

4(d), removing either GCL or DSM led to a modest increase in RMSE (although their RMSE levels are still lower than the RMSE of no pretrain), indicating that both of them play a crucial role in capturing meaningful representations and improving performance. We also added an ablation study on our two-category graph contrastive loss. We pre-trained two models, one model with two-category contrastive loss (both decoy negative samples and different complexes as negative samples, denoted as “with two-category graph contrastive loss”) and the other with one-category GCL loss (only different complexes as negative samples, denoted as “without decoy samples”). Results in Table 3 show that the proposed two-category graph contrastive loss slightly outperforms a one-category contrastive loss on both datasets.

5.4 Varying Label Sizes in Fine-Tuning

We also assessed the effect of our pre-training on sample efficiency and learning efficiency during fine-tuning, especially when the amount of labels is limited. We changed the number of labeled samples from 2000 to 12000 during fine-tuning. As shown in Figure 4(c), the pre-trained model consistently achieves lower RMSEs across all label sizes, with the most notable improvements observed with fewer labeled samples (lower mean RMSE and smaller variance). Moreover, pre-training appears to accelerate the convergence during the fine-tuning phase. To confirm this, we used an early stopping mechanism with a patience of 10 epochs. Figure 4(d) shows that the pre-trained model not only starts with a lower initial RMSE but also reaches convergence more quickly (around 20 epochs) compared to the base model without our pre-training (over 40 epochs). This confirms that our pretraining enhances the label sample efficiency during fine-tuning.

5.5 Generalization

It has been shown that the default split of general (training), refined (validation), and core (test) datasets in PDBbind is cross-contaminated with proteins and ligands with high similarity. To rigorously evaluate the effect of our pretraining on a model’s generalizability, we used a leakage-proof split called LP-PDBbind [Li *et al.*, 2024a], which partitions PDBbind into training (10980 samples), validation (2312 samples), and test (4651 samples) sets based on high sequence and structural similarity across proteins and ligands. As a comparison, we also randomly split the data into training, validation, and test sets with the same sizes. The experimental results in Table 4 on the GIGN base model show a much more significant improvement after pretraining on the LP-PDBbind compared with a random split. This indicates that our pretraining framework enhances the generalizability of a base model across different protein and ligand structures.

Table 4: Model generalizability test on a leakage-proof split (LP-PDBbind)

	No pre-train	Pre-train
LP-PDBbind split	1.496 (0.029)	1.371 (0.006)
Random split	1.294 (0.017)	1.269 (0.015)

6 Conclusion and Future Works

In this paper, we propose *DecoyDB*, a comprehensive dataset of high-resolution 3D complexes augmented with decoys for pretraining graph neural networks in protein-ligand binding affinity prediction. We also design a customized GCL algorithm based on DecoyDB. Experiments show that pre-training on DecoyDB improves multiple base models in prediction accuracy, sample learning efficiency, and model generalizability.

In the future, we plan to extend the proposed framework to other tasks beyond binding affinity prediction, such as binding pose estimation and drug generation.

References

- Helen M. Berman, John Westbrook, Zukang Feng, Gary Gilliland, T. N. Bhat, Helge Weissig, Ilya N. Shindyalov, and Philip E. Bourne. The protein data bank. *Nucleic Acids Research*, 28(1):235–242, 01 2000.
- Ting Chen, Simon Kornblith, Mohammad Norouzi, and Geoffrey Hinton. A simple framework for contrastive learning of visual representations. In *International conference on machine learning*, pages 1597–1607. PMLR, 2020.
- Mindy I Davis, Jeremy P Hunt, Sanna Herrgard, Pietro Ciceri, Lisa M Wodicka, Gabriel Pallares, Michael Hocker, Daniel K Treiber, and Patrick P Zarrinkar. Comprehensive analysis of kinase inhibitor selectivity. *Nature biotechnology*, 29(11):1046–1051, 2011.
- Jerome Eberhardt, Diogo Santos-Martins, Andreas F Tillack, and Stefano Forli. Autodock vina 1.2. 0: New docking methods, expanded force field, and python bindings. *Journal of chemical information and modeling*, 61(8):3891–3898, 2021.
- Yin Fang, Qiang Zhang, Ningyu Zhang, Zhuo Chen, Xiang Zhuang, Xin Shao, Xiaohui Fan, and Huajun Chen. Knowledge graph-enhanced molecular contrastive learning with functional prompt. *Nature Machine Intelligence*, 5(5):542–553, 2023.
- Evan N Feinberg, Debnil Sur, Zhenqin Wu, Brooke E Husic, Huanghao Mai, Yang Li, Saisai Sun, Jianyi Yang, Bharath Ramsundar, and Vijay S Pande. Potentialnet for molecular property prediction. *ACS central science*, 4(11):1520–1530, 2018.
- Paul G Francoeur, Tomohide Masuda, Jocelyn Sunseri, Andrew Jia, Richard B Iovanisci, Ian Snyder, and David R Koes. Three-dimensional convolutional neural networks and a cross-docked data set for structure-based drug design. *Journal of chemical information and modeling*, 60(9):4200–4215, 2020.
- Samuel Genheden and Ulf Ryde. The mm/pbsa and mm/gbsa methods to estimate ligand-binding affinities. *Expert opinion on drug discovery*, 10(5):449–461, 2015.
- Xiaoyu Guan and Daoqiang Zhang. T-mgcl: Molecule graph contrastive learning based on transformer for molecular property prediction. *IEEE/ACM Transactions on Computational Biology and Bioinformatics*, 2023.
- Kaiming He, Haoqi Fan, Yuxin Wu, Saining Xie, and Ross Girshick. Momentum contrast for unsupervised visual representation learning. In *Proceedings of the IEEE/CVF conference on computer vision and pattern recognition*, pages 9729–9738, 2020.
- Kaiming He, Xinlei Chen, Saining Xie, Yanghao Li, Piotr Dollár, and Ross Girshick. Masked autoencoders are scalable vision learners. In *Proceedings of the IEEE/CVF conference on computer vision and pattern recognition*, pages 16000–16009, 2022.
- Dejun Jiang, Chang-Yu Hsieh, Zhenxing Wu, Yu Kang, Jike Wang, Ercheng Wang, Ben Liao, Chao Shen, Lei Xu, Jian Wu, Dongsheng Cao, and Tingjun Hou. Interactiongraphnet: A novel and efficient deep graph representation learning framework for accurate protein–ligand interaction predictions. *Journal of Medicinal Chemistry*, 64(24):18209–18232, 2021. PMID: 34878785.
- Wengong Jin, Siranush Sarkizova, Xun Chen, Nir Hacoheh, and Caroline Uhler. Unsupervised protein-ligand binding energy prediction via neural euler’s rotation equation. *Advances in Neural Information Processing Systems*, 36, 2024.
- John G Kirkwood. Statistical mechanics of fluid mixtures. *The Journal of chemical physics*, 3(5):300–313, 1935.
- Douglas B Kitchen, Hélène Decornez, John R Furr, and Jürgen Bajorath. Docking and scoring in virtual screening for drug discovery: methods and applications. *Nature reviews Drug discovery*, 3(11):935–949, 2004.

- Mark Lennox, Neil Robertson, and Barry Devereux. Modelling drug-target binding affinity using a bert based graph neural network. *Annual International Conference of the IEEE Engineering in Medicine and Biology Society. IEEE Engineering in Medicine and Biology Society. Annual International Conference*, page 4348–4353, November 2021.
- Y. Li, M. A. Rezaei, C. Li, and X. Li. Deepatom: A framework for protein-ligand binding affinity prediction. In *2019 IEEE International Conference on Bioinformatics and Biomedicine (BIBM)*, pages 303–310, nov 2019.
- Hongjian Li, Kam-Heung Sze, Gang Lu, and Pedro J Ballester. Machine-learning scoring functions for structure-based drug lead optimization. *Wiley Interdisciplinary Reviews: Computational Molecular Science*, 10(5):e1465, 2020.
- Shuangli Li, Jingbo Zhou, Tong Xu, Dejing Dou, and Hui Xiong. Geomgcl: Geometric graph contrastive learning for molecular property prediction. In *Proceedings of the AAAI conference on artificial intelligence*, volume 36, pages 4541–4549, 2022.
- Yanjun Li, Daohong Zhou, Guangrong Zheng, Xiaolin Li, Dapeng Wu, and Yaxia Yuan. Dyscore: A boosting scoring method with dynamic properties for identifying true binders and nonbinders in structure-based drug discovery. *Journal of chemical information and modeling*, 62(22):5550–5567, 2022.
- Jie Li, Xingyi Guan, Oufan Zhang, Kunyang Sun, Yingze Wang, Dorian Bagni, and Teresa Head-Gordon. Leak proof pdbbind: a reorganized dataset of protein-ligand complexes for more generalizable binding affinity prediction. *ArXiv*, pages arXiv–2308, 2024.
- Xuelian Li, Cheng Shen, Hui Zhu, Yujian Yang, Qing Wang, Jincal Yang, and Niu Huang. A high-quality data set of protein–ligand binding interactions via comparative complex structure modeling. *Journal of Chemical Information and Modeling*, 64(7):2454–2466, 2024.
- Jaechang Lim, Seongok Ryu, Kyubyong Park, Yo Joong Choe, Jiyeon Ham, and Woo Youn Kim. Predicting drug–target interaction using a novel graph neural network with 3d structure-embedded graph representation. *Journal of Chemical Information and Modeling*, 59(9):3981–3988, 2019. PMID: 31443612.
- Tiqing Liu, Yuhmei Lin, Xin Wen, Robert N Jorissen, and Michael K Gilson. Bindingdb: a web-accessible database of experimentally determined protein–ligand binding affinities. *Nucleic acids research*, 35(suppl_1):D198–D201, 2007.
- Maotao Liu, Yifan Yang, Xu Gong, Li Liu, and Qun Liu. Hiermrl: Hierarchical structure-aware molecular representation learning for property prediction. In *2022 IEEE International Conference on Bioinformatics and Biomedicine (BIBM)*, pages 386–389. IEEE, 2022.
- Zemin Liu, Xingtong Yu, Yuan Fang, and Xinming Zhang. Graphprompt: Unifying pre-training and downstream tasks for graph neural networks. In *Proceedings of the ACM web conference 2023*, pages 417–428, 2023.
- Ding Luo, Dandan Liu, Xiaoyang Qu, Lina Dong, and Binju Wang. Enhancing generalizability in protein–ligand binding affinity prediction with multimodal contrastive learning. *Journal of Chemical Information and Modeling*, 64(6):1892–1906, 2024.
- Gabriele Macari, Daniele Toti, Andrea Pasquadibisceglie, and Fabio Polticelli. Dockingapp rf: a state-of-the-art novel scoring function for molecular docking in a user-friendly interface to autodock vina. *International Journal of Molecular Sciences*, 21(24):9548, 2020.
- Maho Nakata and Tomomi Shimazaki. Pubchemqc project: a large-scale first-principles electronic structure database for data-driven chemistry. *Journal of chemical information and modeling*, 57(6):1300–1308, 2017.
- Thin Nguyen, Hang Le, Thomas P Quinn, Tri Nguyen, Thuc Duy Le, and Svetha Venkatesh. GraphDTA: predicting drug–target binding affinity with graph neural networks. *Bioinformatics*, 37(8):1140–1147, 10 2020.

- Yuyan Ni, Shikun Feng, Xin Hong, Yuancheng Sun, Wei-Ying Ma, Zhi-Ming Ma, Qiwei Ye, and Yanyan Lan. Pre-training with fractional denoising to enhance molecular property prediction. *Nature Machine Intelligence*, 6(10):1169–1178, 2024.
- Jiayu Qin, Jian Chen, Rohan Sharma, Jingchen Sun, and Changyou Chen. A probability contrastive learning framework for 3d molecular representation learning. In *The Thirty-eighth Annual Conference on Neural Information Processing Systems*, 2024.
- Alec Radford, Karthik Narasimhan, Tim Salimans, Ilya Sutskever, et al. Improving language understanding by generative pre-training. 2018.
- Mohammad A Rezaei, Yanjun Li, Dapeng Wu, Xiaolin Li, and Chenglong Li. Deep learning in drug design: Protein-ligand binding affinity prediction. *IEEE/ACM Transactions on Computational Biology and Bioinformatics*, 19(01):407–417, 2022.
- Victor Garcia Satorras, Emiel Hoogeboom, and Max Welling. E (n) equivariant graph neural networks. In *International conference on machine learning*, pages 9323–9332. PMLR, 2021.
- Kristof Schütt, Pieter-Jan Kindermans, Huziel Enoc Saucedo Felix, Stefan Chmiela, Alexandre Tkatchenko, and Klaus-Robert Müller. Schnet: A continuous-filter convolutional neural network for modeling quantum interactions. In I. Guyon, U. Von Luxburg, S. Bengio, H. Wallach, R. Fergus, S. Vishwanathan, and R. Garnett, editors, *Advances in Neural Information Processing Systems*, volume 30. Curran Associates, Inc., 2017.
- Till Siebenmorgen, Filipe Menezes, Sabrina Benassou, Erinc Merdivan, Kieran Didi, André Santos Dias Mourão, Radosław Kitel, Pietro Liò, Stefan Kesselheim, Marie Piraud, et al. Misato: machine learning dataset of protein–ligand complexes for structure-based drug discovery. *Nature Computational Science*, pages 1–12, 2024.
- Marta M Stepniewska-Dziubinska, Piotr Zielenkiewicz, and Pawel Siedlecki. Development and evaluation of a deep learning model for protein–ligand binding affinity prediction. *Bioinformatics*, 34(21):3666–3674, 2018.
- Marta M Stepniewska-Dziubinska, Piotr Zielenkiewicz, and Pawel Siedlecki. Development and evaluation of a deep learning model for protein–ligand binding affinity prediction. *Bioinformatics*, 34(21):3666–3674, 05 2018.
- Mengying Sun, Jing Xing, Huijun Wang, Bin Chen, and Jiayu Zhou. Mocl: data-driven molecular fingerprint via knowledge-aware contrastive learning from molecular graph. In *Proceedings of the 27th ACM SIGKDD conference on knowledge discovery & data mining*, pages 3585–3594, 2021.
- Jing Tang, Agnieszka Szwejda, Sushil Shakyawar, Tao Xu, Petteri Hintsanen, Krister Wennerberg, and Tero Aittokallio. Making sense of large-scale kinase inhibitor bioactivity data sets: a comparative and integrative analysis. *Journal of chemical information and modeling*, 54(3):735–743, 2014.
- Philipp Thölke and Gianni De Fabritiis. Equivariant transformers for neural network based molecular potentials. In *International Conference on Learning Representations*, 2022.
- Zekun Tong, Yuxuan Liang, Henghui Ding, Yongxing Dai, Xinke Li, and Changhu Wang. Directed graph contrastive learning. *Advances in neural information processing systems*, 34:19580–19593, 2021.
- Swapnil Wagle, Richard D Smith, Anthony J Dominic III, Debarati DasGupta, Sunil Kumar Tripathi, and Heather A Carlson. Sunseting binding moad with its last data update and the addition of 3d-ligand polypharmacology tools. *Scientific Reports*, 13(1):3008, 2023.
- Xiao Wang and Guo-Jun Qi. Contrastive learning with stronger augmentations. *IEEE transactions on pattern analysis and machine intelligence*, 45(5):5549–5560, 2022.
- Renxiao Wang, Xueliang Fang, Yipin Lu, Chao-Yie Yang, and Shaomeng Wang. The pddbnd database: methodologies and updates. *Journal of medicinal chemistry*, 48(12):4111–4119, 2005.
- Yingze Wang, Kunyang Sun, Jie Li, Xingyi Guan, Oufan Zhang, Dorian Bagni, Yang Zhang, Heather A Carlson, and Teresa Head-Gordon. A workflow to create a high-quality protein–ligand binding dataset for training, validation, and prediction tasks. *Digital Discovery*, 2025.

- Fang Wu, Shuting Jin, Yinghui Jiang, Xurui Jin, Bowen Tang, Zhangming Niu, Xiangrong Liu, Qiang Zhang, Xiangxiang Zeng, and Stan Z Li. Pre-training of equivariant graph matching networks with conformation flexibility for drug binding. *Advanced Science*, 9(33):2203796, 2022.
- Dongkuan Xu, Wei Cheng, Dongsheng Luo, Haifeng Chen, and Xiang Zhang. Infogcl: Information-aware graph contrastive learning. *Advances in Neural Information Processing Systems*, 34:30414–30425, 2021.
- Jianyi Yang, Amrisha Roy, and Yang Zhang. Biolip: a semi-manually curated database for biologically relevant ligand–protein interactions. *Nucleic acids research*, 41(D1):D1096–D1103, 2012.
- Ziduo Yang, Weihe Zhong, Qiujie Lv, Tiejun Dong, and Calvin Yu-Chian Chen. Geometric interaction graph neural network for predicting protein–ligand binding affinities from 3d structures (gign). *The journal of physical chemistry letters*, 14(8):2020–2033, 2023.
- Yuning You, Tianlong Chen, Yongduo Sui, Ting Chen, Zhangyang Wang, and Yang Shen. Graph contrastive learning with augmentations. *Advances in neural information processing systems*, 33:5812–5823, 2020.
- Sheheryar Zaidi, Michael Schaarschmidt, James Martens, Hyunjik Kim, Yee Whye Teh, Alvaro Sanchez-Gonzalez, Peter Battaglia, Razvan Pascanu, and Jonathan Godwin. Pre-training via denoising for molecular property prediction. In *The Eleventh International Conference on Learning Representations*, 2023.
- Yunjiang Zhang, Shuyuan Li, Kong Meng, and Shaorui Sun. Machine learning for sequence and structure-based protein–ligand interaction prediction. *Journal of Chemical Information and Modeling*, 64(5):1456–1472, 2024.
- Liangzhen Zheng, Jingrong Fan, and Yuguang Mu. Onionnet: a multiple-layer intermolecular-contact-based convolutional neural network for protein–ligand binding affinity prediction. *ACS omega*, 4(14):15956–15965, 2019.
- Robert W Zwanzig. High-temperature equation of state by a perturbation method. i. nonpolar gases. *The Journal of Chemical Physics*, 22(8):1420–1426, 1954.

A Experiment Setup

A.1 Evaluation metrics

In this section, we provide the details about our two evaluation metrics in our experiment. Root Mean Square Error (RMSE) and Pearson’s correlation coefficient (R) are denoted as:

$$RMSE = \sqrt{\frac{1}{N} \sum_{i=1}^N (y_i - \hat{y}_i)^2} \quad (6)$$

$$R = \frac{\sum_{i=1}^N (y_i - \bar{y})(\hat{y}_i - \bar{\hat{y}})}{\sqrt{\sum_{i=1}^N (y_i - \bar{y})^2 \sum_{i=1}^N (\hat{y}_i - \bar{\hat{y}})^2}} \quad (7)$$

y_i and \hat{y}_i represents experimental and predicted binding affinity, respectively.

A.2 Data Preprocessing

The edges E_k between atoms can be determined by the chemical bonds (covalent bonds) or a distance threshold. In our case, we used a distance threshold (5\AA) to establish edges within the protein and the interactive edges between protein atoms and ligand atoms. We used the same distance threshold to filter out relevant atoms within protein binding pockets for the graphs. We kept the covalent bonds within a ligand as ligand edges.

A.3 Training Parameters

In our experiments, we trained and evaluated the DeepDTA, GraphDTA, Pafnucy, OnionNet, SchNet, EGNN, TorchMD-Net and GIGN models. The Adam optimizer was employed for all models with the following settings: the initial learning rate was set to 5×10^{-4} , weight decay was set to 1×10^{-6} . To prevent overfitting and enhance the generalization ability of the models, we reduced the learning rate by a factor of 0.1 whenever the performance on the validation set did not improve for 10 consecutive epochs. Additionally, an early stopping strategy was adopted for all models, where training was terminated if the validation performance did not improve within 40 consecutive epochs. The pretraining phase for each model was set to 20 epochs, while the maximum number of epochs for the fine-tuning phase was set to 300. In the fine-tuning phase, we set the batch size to 128. In the pre-training phase, we set the batch size to 8. Each sample in the batch contained 21 structures: 1 real data sample, 10 randomly selected decoys, and 10 perturbed data samples generated by adding Gaussian noise. In addition to performance improvements, we also examined the time cost of our framework. Using GIGN as an example, the pre-training stage took approximately 23 hours, while the fine-tuning stage required only about 30 minutes.

A.4 Model Architecture Parameters

In our experiments, we used the following parameter settings for the baseline models to ensure optimal performance. For Pafnucy, we set the channels of the three-layer 3D convolutions to 64, 128, and 256, respectively. For OnionNet, the input features were set to 3840, and there are 3 convolutional layers with 32, 64, and 128 filters. The kernel size was set to 4. The maximum length of protein sequences in DTA method was set to 1000. SchNet was configured with 3 interaction layers, each having an embedding dimension of 128. Both EGNN and GIGN models utilized a three-layer architecture with each layer having a dimension of 256. For TorchNet-MD, there are 6 layers and each is layer with 256 dimension embedding.

B Baseline models

- **Docking Method: AutoDock Vina** [Eberhardt *et al.*, 2021] is a widely used program for molecular docking, which can also predict binding affinity. Since it is not a deep learning model, we directly cite the results from [Macari *et al.*, 2020]. Note that there are no repeated experiments, so there is no standard error being reported.

- **Drug-Target Affinity (DTA) methods: DeepDTA** [Lennox *et al.*, 2021] predict binding affinity based on protein and ligand sequences separately without interaction networks. **GraphDTA** [Nguyen *et al.*, 2020] is similar to DeepDTA but uses a GNN.
- **CNN-based methods: Pafnucy** [Stepniewska-Dziubinska *et al.*, 2018b] is a 3D-CNN model. **OnionNet** [Zheng *et al.*, 2019] uses 2D-CNN to learn representations.
- **GNN-based methods: TorchMD-Net** [Thölke and De Fabritiis, 2022] is a GNN-based model specially designed for the force field. **SchNet** [Schütt *et al.*, 2017] is a GNN model based on essential quantum chemical constraints. **EGNN** [Satorras *et al.*, 2021] is a GNN based on rotation and translation equivariance. **GIGN** [Yang *et al.*, 2023] is a GNN specifically designed for protein-ligand interactions. This is among the state of the art methods.
- **Pre-training for general graphs:** General **GCL** based on edge perturbation and node dropping. We only tested these methods on top of the best baseline GNN model GIGN, including GCL with edge perturbation (GIGN+GCL-EP) or node dropping (GIGN+GCL-ND).
- **Pre-training for biochemistry graphs:** (1) **Frad** [Ni *et al.*, 2024] designed a chemical-guided noise and utilizes denoising for pretraining. We only evaluated Frad on top of TorchMD-Net due to the availability of source codes. (2) **ConBAP** [Luo *et al.*, 2024] designs a contrastive learning strategy based on (binary) negative samples from decoys. We only evaluated ConBAP on EGNN due to the availability of source codes.
- **OURS:** This is our proposed graph contrastive learning framework. We evaluated our framework on top of GIGN, EGNN, and SchNet.

C Pseudo code

We summarize our framework in Algorithm 1 and 2.

Algorithm 1 Graph Contrastive Pretraining

- 1: **Input:** Protein-ligand complexes \mathcal{S} , a GNN encoder f_θ
 - 2: **Output:** Pretrained parameters θ of encoder f_θ
 - 3: **for** each unlabeled protein-ligand complex in \mathcal{S} **do**
 - 4: Identify positive and two-category negative pairs
 - 5: Compute latent representation $\mathbf{z} = f_\theta(s)$ for them
 - 6: Compute contrastive loss L_1 (Equation 3)
 - 7: Sample gaussian noise ϵ
 - 8: Apply noise to ligand coordinates: $\mathbf{x}' = \mathbf{x} + \epsilon$
 - 9: Compute denoising loss L_2 (Equation 4)
 - 10: Compute total loss: \mathcal{L} (Equation 5)
 - 11: Update encoder parameters: $\theta \leftarrow \theta - \eta \nabla_\theta \mathcal{L}$
 - 12: **end for**
-

Algorithm 2 Finetuning

- 1: **Input:** Pretrained encoder f_θ , labeled protein-ligand complexes S_l and a new regression head g_ϕ
s.t. $\hat{y}_k = g_\phi(f_\theta(s_k))$
 - 2: **Output:** Fine-tuned parameters θ and ϕ
 - 3: Replace regression head g_ϕ
 - 4: **for** each labeled protein-ligand complex s_k in S_l **do**
 - 5: Predict binding affinity: $\hat{y} = g_\phi(f_\theta(s_k))$
 - 6: Compute loss: $\mathcal{L}_{\text{finetune}} = \frac{1}{N} \sum_{i=1}^N (\hat{y}_i - y_i)^2$
 - 7: Update parameters: $[\theta, \phi] \leftarrow [\theta, \phi] - \eta \nabla_{\theta, \phi} \mathcal{L}_{\text{finetune}}$
 - 8: **end for**
-